Boise State University

ScholarWorks

Materials Science and Engineering Faculty Publications and Presentations

Micron School for Materials Science and Engineering

1-2010

Microstructural Effects During Chemical Mechanical Planarization of Copper

Patrick J. Andersen
Boise State University

Mariela N. Bentancur
Boise State University

Amy J. Moll
Boise State University

Megan Frary
Boise State University

© The Electrochemical Society, Inc. 2010. All rights reserved. Except as provided under U.S. copyright law, this work may not be reproduced, resold, distributed, or modified without the express permission of the Electrochemical Society (ECS). The archival version of this work was published in *Journal of the Electrochemical Society*, 157(1), H120-H126. DOI: 10.1149/1.3254163

Manuscript published in the Journal of The Electrochemical Society, **157** H120-H126 (2010)

Microstructural Effects during Chemical Mechanical Planarization of Copper

Patrick J. Andersen, Mariela N. Bentancur, Amy J. Moll, Megan Frary
Department of Materials Science and Engineering, Boise State University
1910 University Drive, Boise, ID 83725-2075

ABSTRACT

Novel die-stacking schema using through-wafer interconnects require vias to be filled with electroplated Cu, resulting in thick copper films, and requiring an aggressive first-step CMP. This work investigates the effects of microstructure on CMP of copper films, which are not presently well understood. Bulk and local removal rates were investigated for several different microstructures. Surface orientation maps were created and the orientations of individual grains were correlated with topographical data to elucidate local removal behavior. Cu removal depends on the details of the microstructure, and certain microstructures allowed for either faster or more uniform removal of thick Cu films.

INTRODUCTION

Chemical mechanical planarization (CMP) is an important step in semiconductor processing that is used to planarize topography and expose features on the surface of a silicon wafer. In the CMP process, the wafer is polished using a slurry which removes material by combined action of chemical and mechanical (i.e., through abrasion) means such that undesirable features including copper overburden are polished off.[1] As the features of interest (e.g., interconnects) have become smaller, more consistent and predictable results from CMP are required. Since copper is the predominant metal used for interconnects, much work has been done to understand how Cu responds to different slurry chemistries, machine variables, and consumables during CMP.[2, 3] One variable that has not received as much attention is the role of the microstructure of the Cu film in the CMP process.

CMP is an important process for advanced packaging solutions including 3-D semiconductor integration. Through-wafer interconnects are an essential component when using stacked chips in a 3-D package.[4] One process for creating three-dimensionally stacked chips uses through-wafer vias filled with copper.[5, 6] In this process, a thick electroplated copper film (~15-30 μm) with significant height variation is left on the surface. A CMP step is required to remove the thick copper film.[7] To improve speed and efficiency, Miranda *et al.* optimized the process using an aggressive slurry formulation to remove a majority of the film.[7] This aggressive step was followed by CMP with a conventional slurry (i.e., one used in the CMP of thin films) to leave an acceptably smooth surface for future processing steps. While the results were satisfactory, no attention was given to the role of microstructure on removal rate or surface height variation. The aggressive first step in the two-part CMP process operates largely by chemical etching and results in significant roughness of the surface (~190 nm) following CMP; the roughness may result from crystallographic anisotropy in copper. The anisotropy could be linked to different rates of removal during CMP [8] and investigation of the crystallographic orientation of the grains close to the surface may provide a better understanding of surface roughness thereafter. For example, if particular orientations show faster removal rates, the height of these grains after CMP would differ from those of neighboring grains.

This is an author-produced, peer-reviewed version of this article. The final, definitive version of this document can be found online published by The Electrochemical Society. Copyright restrictions may apply. doi: 10.1149/1.3254163

Several properties of copper exhibit anisotropy and may affect surface height variation and removal rate during CMP. For instance, anisotropy of hardness and mechanical wear [9, 10] could affect the tribological response of copper to CMP.[11] Chemical etch rate and surface energy anisotropy [12-14] lead to different chemical responses of copper to CMP. These anisotropies could be observed by the response of individual grains and of individual grain boundaries to CMP. It is expected that grains with different orientations and grain boundaries of varying character will have different responses to CMP. On the other hand, observations could be made more broadly, where crystallographic texture, grain size, and grain boundary character distribution may affect bulk removal rate and surface uniformity.

The texture of the Cu film is, in part, controlled by processing conditions during electroplating; variations in grain size, crystallographic texture, and grain boundary character distribution arise due to differences in bath chemistry, current, waveform, and solution temperature.[15] In addition, post-plating thermal treatments to accelerate stress-relaxation affect the final microstructure.[16] A crystallographic texture with significant resistance to mechanical wear would have much lower CMP removal rates than a texture with a different orientation that has much lower resistance to mechanical wear.[17] Additionally, grain boundaries are high energy interfaces between grains and often etch or corrode at a higher rate than the rest of the surface. As a smaller grain size results in a greater total grain boundary length for a given area, the total energy of the system may be increased. The role of grain boundaries during CMP is further complicated by the fact that grain boundary energy depends on the structure of the boundary (e.g., its misorientation).[18] Therefore, both the grain size and the distribution of grain boundary types are expected to play separate, but interconnected, roles in determining bulk removal rate during CMP.

The effect of the microstructure of copper thin films on conventional CMP processes has been investigated,[16, 19-22] but there has been little work on thick films. For example, Ni *et al*. studied post-CMP surface roughness in samples with twinned or equiaxed grains.[20] They found that the highly twinned sample had significantly greater roughness than the equiaxed sample because of the alternating grain orientations. The higher surface energy of the less favorably oriented twin grain resulted in greater local copper removal. Therefore, because the twinned sample had alternating favorably and unfavorably oriented grains adjacent to one another, the surface was unacceptably rough. In contrast, the equiaxed sample had smooth transitions between the grains and an acceptable roughness.[20] While Ni's work is relevant to the microstructural effects expected in thick copper films, their work was on copper films with very small grain sizes and focused on very low surface roughness values. In thick films, there is a potential for larger grain sizes and crystallographic textures which are not solely dependent on film thickness.[23] As described above, plating conditions influence the film microstructure, as does the feature size of the via. When filling the 3-D vias, a much thicker Cu film tends to form as compared with Cu deposition for 2-D features.[7]

Another microstructural effect that has been explored in the CMP of thin copper films is the relationship between the removal rate and grain size or hardness.[16, 24] In one study of narrow damascene Cu interconnects, Ernur *et al.* found that grain size influenced the etch rate as did the slurry chemistry; smaller grains etched faster than did large grains in inorganic acids, but the larger grains etched faster in organic solutions.[24] Although the work of Ernur *et al.* did investigate the effects of grain size, they did so for narrow 2-D interconnects and did not

This is an author-produced, peer-reviewed version of this article. The final, definitive version of this document can be found online published by The Electrochemical Society. Copyright restrictions may apply. doi: 10.1149/1.3254163

consider what happens in the film structures that result from filling 3-D vias; they also did not account for the effects of crystallographic texture.

Although the studies just described consider the effects of some microstructural variables on CMP, only a few known studies have examined the relationship between surface orientation and CMP behavior. For thin Cu films (1 μm thick), Feng *et al.*[17] found that a higher ratio of (111) to (200) surfaces promoted a lower overall CMP removal rate. They suggest that (111) surfaces minimize surface energy which would lead to slower Cu removal. In the case of sapphire, Zhu *et al.* [25] found that (0001) planes had much greater removal rates than did $(11\bar{2}0)$or $(10\bar{1}0)$ surfaces. They attributed the result to the formation of a soft hydration layer on the (0001) plane that facilitates material removal.[25] Beyond these studies, no known work has been done to quantify the effects of local grain orientations from within the entire spectrum on CMP behavior. One method to quantify anisotropic surface phenomena was presented by Schuh *et al.* who correlated crystallographic data obtained by electron backscatter diffraction (EBSD) with surface relief data from atomic force microscopy (AFM).[26] The advantage of this technique is that the effects of orientation on surface phenomena can be determined for the entire spectrum of surface orientations. In the present work, the technique developed by Schuh *et al.*[26] is used to explore the effects of microstructural variables on both the bulk and local removal behavior for thick copper films. By correlating local CMP removal parameters (e.g., removal rate) to microstructural properties such as grain size and crystallographic texture, methods to tailor either CMP or copper plating and annealing processes to optimize the removal of thick copper films may result.

EXPERIMENTAL PROCEDURES

Experimental materials

In the present study of microstructural effects on CMP, two different types of specimens were used. The first set of specimens were thin copper sheets (thickness = 0.5 mm, purity = 99.9%) cold rolled and machined into disks (diameter = 100 mm). In order to study the effects of grain size on CMP, the solid Cu disks were annealed at 650°C for 0.5, 4, or 16 h in air. For the second type of specimens, Cu films (~ 20 μm thick) were electroplated onto Si wafers 100 mm in diameter at Research Triangle Inc. (RTI, Research Triangle, NC).[27] Prior to electrodeposition of Cu, a 3 nm thick Cu seed-layer was deposited by physical vapor deposition. Electrodeposition of Cu films occurred in a Technic Cu3300 bath at 25°C for 50 minutes. Both direct and pulsed current were used; the direct current density was 27, 32, or 53 mA/cm². One sample was also produced using 32 mA/cm² current density and a 91% duty cycle, where plating current was applied for 10 ms over an 11 ms interval (i.e., 10 ms on, 1 ms off). A proprietary polarizer additive, also provided by Technic, was added to the plating bath in varying concentrations (0, 1 or 7 mL/L) during sample preparation. In this study, the different currents used did not significantly affect the resulting microstructure, but the polarizer content did result in microstructural differences. After plating, samples were annealed for 2 h at 400°C to create microstructures with varying grain sizes. Before CMP, the average roughness of the electroplated wafers was measured with optical profilometry to determine the "flatness" of the surface. In general, the average roughness was ~ 20 nm for the plated Cu films.

This is an author-produced, peer-reviewed version of this article. The final, definitive version of this document can be found online published by The Electrochemical Society. Copyright restrictions may apply. doi: 10.1149/1.3254163

Chemical-mechanical planarization

After annealing, both sets of specimens (solid Cu disks and Cu-plated wafers) underwent chemical-mechanical planarization using a Strasbaugh 6DS-SP CMP tool (San Luis Obispo, CA) using identical operating parameters. The CMP processing used an XY-grooved Thomas West STT™W711 (Sunnyvale, CA) pad and the machine parameters for all tests were: down pressure = 20.7 kPa, spindle speed = 60 rpm, table speed = 60 rpm, and total slurry flow rate of 150 mL/min. An aggressive slurry (Fujimi DCM-M42, Tualatin, OR) with a strong chemical etching component was used to produce a high removal rate for thick films. Cu-plated wafers were processed by CMP for 15 s, and the solid Cu disks were processed for 30 s. The CMP processing parameters were based on previous work [7] and recommendations from the slurry manufacturer. The overall Cu removal rate was determined by weighing the specimens (Ohaus Adventurer AR2140 analytical balance, resolution = 0.0001 g) before and after CMP and assuming fully dense Cu. After CMP, the wafers were sectioned into small squares for SEM and EBSD analysis.

Microstructural characterization

To determine the effects of orientation on local removal rate and surface height variation, the surface topography was imaged after CMP using two different techniques that allow for analysis of areas of different sizes. The first technique used an AFM (Veeco Dimension 3100, Nanoscope IV controller, Santa Barbara, CA) equipped with an X-Y closed loop scanner and Nanosensors PointProbe-Plus non-contact n-doped silicon tips. Imaging was performed under dry conditions in tapping mode with a resonant frequency of 204 to 497 kHz and a force constant of 10 to 130 N/m. AFM images were analyzed using the Nanoscope software. The second surface mapping technique was optical profilometry using a Wyko NT100 microscope (Veeco Metrology Inc., Tucson, AZ) Surface height was measured using the vertical scanning interferometry mode with a 50× objective. Height and surface roughness data were processed using Veeco Vision 32 for NT-1100 software. AFM was used primarily on electroplated samples because grain size and surface roughness were within its operating range. Optical profilometry was used on solid Cu disks to accommodate their larger grain size and surface height range. Surface topography data were collected in areas referenced by fiducial markers created with a Vicker's hardness tester.

After characterizing the surface topography that results from CMP, the next step was to characterize the crystallographic orientation of the surface in the same areas; using the fiducial markers as guides, maps of the same areas were then correlated to extract the relationship between orientation and local removal rate. Surface orientation was characterized using EBSD which determines the crystallographic orientation of the surface by indexing diffraction patterns generated in the SEM. Prior to EBSD analysis, all samples were electropolished with concentrated phosphoric acid for 3 minutes at 0.02 A at 25°C. The EBSD system (EDAX/TSL, Draper, UT) is mounted on a LEO 1430VP SEM. During EBSD, the operating voltage is 25 kV and the working distance is between 11 and 18 mm. EBSD data were collected using a step size of 0.15-0.25 μm on a hexagonal grid for areas between 50×50 to 100×100 μm^2. OIM Analysis software (version 4.6) was used to clean the data set; one pass of the grain confidence index standardization was used with a grain tolerance angle of 5° and a minimum grain size of 2 pixels followed by two passes of neighbor orientation correlation. Grain size and texture were determined using the EBSD software. Texture calculations used a harmonic series expansion with a series rank L = 24 and a Gaussian half-width equal to 5°.

This is an author-produced, peer-reviewed version of this article. The final, definitive version of this document can be found online published by The Electrochemical Society. Copyright restrictions may apply. doi: 10.1149/1.3254163

RESULTS

Microstructural Characterization of Experimental Materials

The grain size, grain boundary character distribution and texture of both types of copper specimens were characterized using EBSD. Figure 1 shows EBSD images taken from the as-received and annealed (16 h) solid Cu disks. The as-received sample (Fig. 1a) has a preferred grain orientation towards the [001] direction with a grain size of about 32 μm. In contrast, the sample annealed for 16 h (Fig. 1b) has a more random crystallographic texture with a grain size of about 85 μm. Figure 2 shows the microstructure of six different electroplated Cu specimens: the images on the left (a, c, and e) are the as-received films, while images on the right (b, d, and f) are for films annealed for 2 h at 400°C. The insets are the (001) pole figures which have the same color scale for all specimens; the maximum is four times the probability of finding a given orientation in a random orientation distribution (4 MRD, multiples of a random distribution). The specimen that does not have polarizer added has a strong [112] fiber texture as seen in the pole figure, with a grain size of about 1.5 μm in the as-plated condition (Fig. 2a) and 7.2 μm after annealing (Fig. 2b). The specimen with 1 mL/L polarizer shows a more random texture (i.e., no preferred orientations), with a grain size of 1.6 μm after plating (Fig. 2c) and 2.9 μm after annealing (Fig. 2d). Finally, the specimen with 7 mL/L of polarizer shows a [111] fiber texture, with a grain size of 2.0 μm in the as-plated condition (Fig. 2e) and 4.8 μm after annealing (Fig. 2f). From the inset pole figures, it is clear that there is very little change, either qualitatively or quantitatively, in the film texture during annealing. With no polarizer (Figs. 2a and 2b), the texture strength changes from 3.96 to 3.93 MRD upon annealing; with 1 mL/L (Figs. 2c and 2d), from 1.99 to 1.97 MRD, and with 7 mL/L (Figs. 2e and 2f), from 2.27 to 2.77 MRD.

Bulk Removal Rate during Chemical Mechanical Planarization

The bulk removal rate was determined by weighing the specimens (both solid Cu disks and Cu-plated wafers) before and after CMP processing. Figure 3 shows the bulk removal rate using undiluted slurry for a Cu-plated wafer and four solid Cu disks as a function of grain size; the error bars correspond to the standard deviation from three different CMP processing trials. As the grain size increases from 6 to 85 μm (corresponding to the Cu-plated wafer and solid Cu disk annealed 16 h), the removal rate increases from 9 to 13 μm/min. By measuring the removal rate from the Cu-plated wafers, which exhibited varying crystallographic textures, the effects of both texture and grain size on bulk removal rate can be determined. Figure 4 shows the removal rate, using diluted slurry to conserve the thinner films, for two of the Cu-plated wafers before and after annealing. In each case, an increase in grain size leads to an increase in removal rate, the same trend observed in Figure 3. Additionally, the results in Figure 4 illustrate the important effect of texture on removal rate. Both the annealed, randomly textured and the as-plated [111]-fiber textured specimens have a grain size of ~3.1 μm; however, the removal rate is about 50% greater in the randomly textured specimen (see Figure 2c). Therefore, it can be concluded from Figure 4 that a stronger <111> texture, as exhibited by the 7 mL/L specimen, leads to a slower bulk removal rate than does a more random texture.

Local Removal Rate during Chemical Mechanical Planarization

In Figure 5, both an EBSD and optical profiler image are shown for a solid Cu disk annealed for 4 h. These two different images are from the same area on the specimen surface and grains can be correlated from one image to the other. While the EBSD map gives grain orientation, the optical profiler map shows the height of the grains after CMP. By comparing the images, we see,

This is an author-produced, peer-reviewed version of this article. The final, definitive version of this document can be found online published by The Electrochemical Society. Copyright restrictions may apply. doi: 10.1149/1.3254163

for example, that the grain labeled E has a darker color in both maps indicating a grain orientation towards the [101] direction and a lower surface height (i.e., more Cu removed). In contrast, grain C is lighter in both maps, indicating an orientation near [111] and less Cu removal. This indicates that grains having a surface normal near the [111] resist removal during CMP better (i.e., these grains are higher in the optical profiler image). Figure 6 shows the relative surface height in μm as a function of the angle between the surface normal and a <111> direction for different annealing times. As the grain orientation deviates from the <111> direction, the local removal rate increases.

In Figure 7, the surface orientation and height are compared for the electroplated Cu films. As in Figure 5, surface orientation is measured by EBSD. However, because the grains are much smaller in the electroplated sample than in the solid Cu disk, AFM was used to measure surface height. After CMP, the average surface roughness for the Cu films is ~240 nm, more than 10 times greater than before CMP. The grain marked with a red circle is lighter in both images which indicates that it is higher relative to other grains and the grain orientation is near the [111] direction. However, the grain marked with an orange circle had more Cu removed and has a surface normal near [101] or [001] which is shown in the EBSD maps. Figure 8 shows the relative surface height as a function of orientation in an inverse pole figure for two different electroplated Cu films. Each point corresponds to a grain; the location gives the orientation while the color indicates the surface height. Figure 8a corresponds to the area in Figure 2a ([112] fiber texture, as-plated) and shows no obvious relationship between orientation and surface height. However, Figure 8b corresponds to the area shown in Figure 2f ([111] fiber texture, annealed 2 h) and shows that grains that have an orientation near [111] resist corrosion better (i.e., points near [111] tend to be purple]. Therefore, we find that the [111] fiber textured specimen shows a clear relationship between orientation and removal rate while the [112] fiber textured specimen does not.

DISCUSSION

Microstructural Characterization of Experimental Materials

The control of texture and grain morphology of electroplated Cu on silicon with plating bath additives was discussed in the previous section. Remarkable control of crystallographic texture was exhibited by altering polarizer (also known as suppressor) concentration as illustrated in Figure 1. Dubin and coworkers [28] make reference to a stronger [111] fiber texture with the addition of bath additive in a similar study using x-ray diffraction. EBSD images in Figure 1 illustrate a similar result, but clearly show that a strong [112] fiber texture developed without polarizer (suppressor) bath additive. Additionally, an intermediate concentration of bath additive causes the development of an almost completely random texture. This unexpected control over texture allowed significantly different microstructures to be created and then linked to bulk and local removal rate data. Although the composition of the polarizer bath additive is unknown, we find that that changing the characteristics of the deposition process leads to different preferred alignments of Cu atoms resulting in different macroscopic crystallographic textures.

Bulk Removal Rate during Chemical Mechanical Planarization

Chemical mechanical planarization is a dynamic process in which the removal of material occurs by both physical (i.e., mechanical) and chemical routes; both routes are directly affected by the microstructure (e.g., the grain size, texture, and grain boundary types) of the material undergoing CMP. As discussed in the results section, the grain size and texture of electroplated Cu can be

This is an author-produced, peer-reviewed version of this article. The final, definitive version of this document can be found online published by The Electrochemical Society. Copyright restrictions may apply. doi: 10.1149/1.3254163

affected by both bath additives and subsequent annealing. Grain size can contribute in two contradictory ways to the bulk removal rate. First, because a larger grained specimen will have a lower hardness, a larger grain size may lead to a faster removal rate through mechanical processes.[29] However, a smaller grained specimen will have more grain boundaries per unit area than the larger grained specimen, and since grain boundaries are susceptible to more aggressive corrosion than the bulk (contributing to the chemical removal process), a smaller grain size could lead to a faster removal rate.[24, 30] By identifying the relationship between removal rate and grain size, the relative importance of each mechanism can be determined. As Figure 3 shows, a larger grain size results in a higher removal rate for the Cu sheet specimens. The same trend is seen in Figure 4 where, regardless of bath additive concentration, annealed samples have higher removal rates than do the as-plated samples with the same plating conditions. To understand the mechanism that drives the removal rate, it is important to remember that the present work is focused on the CMP of thicker Cu films using a more aggressive slurry than is required for CMP of fine damascene lines which results in much higher removal rates. In a typical CMP process, only a small amount of Cu needs to be removed. Therefore, the process is designed to optimize flatness and removal rates are much slower than in the process described in this paper. At slower removal rates, the grain boundaries may have a bigger impact in the overall process due to the mechanism of material removal.[24] However, at the higher removal rates required during CMP of thick films, it is expected that the hardness of the surface is more important in determining the overall behavior.

By comparing specimens with nearly identical grain sizes but with different textures, the effect of texture on the bulk removal rate is identified. Differences in microstructural texture will lead to different responses during the chemical removal process. For example, the annealed sample with the more random texture has approximately the same grain size (d = 3.17 um) as the as-plated sample with a [111] fiber texture (d = 3.10 um), but the removal rate is higher for the more randomly textured sample. In Cu, the (111) plane (i.e., corresponding to grains with [111] surface normals) is known to have the lowest surface energy.[12, 14] As a result, the corrosion rate of [111]-oriented grains is expected to be lower than for other surfaces resulting in a lower observed removal rate. Grains with surface normals of [111] have also been shown to have different mechanical properties than either [001] or [011] grains.[31-33] This finding may also explain the results seen here. If [111]-oriented grains have greater hardness, they will not only resist removal from chemical attack, but will be more mechanically resistant as well. Furthermore, a sample with a strong (i.e., highly non-random) crystallographic texture is more likely to have a higher population of lower energy low-angle grain boundaries, resulting in decreased chemical attack at grain boundaries.[34] From the results in Figures 3 and 4, it is clear that changes in the microstructure, which can be controlled through the processing route, lead to predictable removal rates. Therefore, for a given microstructure, which is usually determined by the application (e.g., to reduce electromigration), an optimized CMP route could be established that takes into account the results presented here on how microstructure affects CMP behavior.

Local Removal Rate during Chemical Mechanical Planarization

The link between individual grain orientation and removal rate was determined by performing CMP on solid copper disks and electroplated wafers, which were then analyzed using the EBSD and surface height analysis. The clearest link between orientation and removal rate is illustrated in Figure 5, where individual grains have relatively flat surfaces whose heights can be measured

This is an author-produced, peer-reviewed version of this article. The final, definitive version of this document can be found online published by The Electrochemical Society. Copyright restrictions may apply. doi: 10.1149/1.3254163

and compared. This comparison is summarized in Figure 6, where, regardless of annealing condition, a general trend of decreasing mean surface height with increasing angular deviation of the surface normal from <111> is found. This result is as expected as lower surface energy (111) grains (i.e., with <111> surface normals) will tend to resist chemical attack better than other orientations.[35-37] Finally, anisotropy in the mechanical properties of copper grain surfaces may cause different responses to abrasion and mechanical wear.[17, 31-33] However, this effect is probably small, because a chemically active slurry with a small abrasive concentration was used in the experiments.

The clear grain by grain correlation in Figure 5 was harder to achieve in the electroplated Cu films due to their small grain size; AFM was required to image the surface topography. One of the reasons that individual grains are harder to resolve in Figure 7 is that the inter-grain interfaces, or grain boundaries, are more susceptible to chemical attack than are the grain interiors. For example, in Figure 5b, the grain edges tend to suffer greater erosion than the grain interiors; however, the extent of the grain boundary attack depends on the crystallographic structure of the boundary. This behavior may be observed more directly in the grain boundary profiles on solid copper disks shown in Figure 9. AFM scans crossing the grain boundary reveal different responses to CMP (i.e., different surface heights) depending on grain boundary structure. In the case of a Σ3 boundary (i.e., a "twin" boundary), the boundary itself shows no sign of attack, although a height difference in the neighboring grains is observed. In the case of a general grain boundary, the grain boundary suffers greater removal of Cu than either of the neighboring grains. If the width of the grain boundary "groove" is comparable to the grain size of the material, there will be no smooth grain interiors as are seen in Figure 5; this results in the undulating surface shown in the surface height plot of Figure 7. In addition to the role that texture and grain size have been found to play, the population of general grain boundaries in the Cu can also influence both the bulk and local removal rates.

The relationship between individual grain orientation and removal rate shown by the solid Cu disks (Figure 6) is also found for the electroplated Cu film with a [111] fiber texture (Figure 8b). Again, grains with surface normal near the [111] direction are more resistant to Cu removal during CMP. In contrast, the electroplated film with a [112] fiber texture (Figure 8a) shows no clear relationship between orientation and removal rate. Therefore, there must be an effect that is more dominant than that driven by surface energy. One possible reason is differences in the distribution of grain boundary types. For example, if the [112] fiber textured film has a higher population of general grain boundaries, which in Figure 9 are seen to be susceptible to erosion, then the height of the grain interiors for small grains could be determined by the grain boundary removal instead of the surface removal rate. In contrast, if the [111] fiber textured film had more low-angle or Σ3 twin boundaries, which are not susceptible to localized erosion, the surface orientation of the grain interiors would dominate the removal rate. Due to the fine grain size and the resolution of EBSD data collection, it is not possible to definitively determine the distribution of grain boundary types. It is clear, however, from Figure 8 that a sharp [111] fiber textured film would result in minimum surface height variation during aggressive CMP of thick Cu because of the uniformity of removal rate for similarly oriented grains.

One important result that emerges from the present work is the influence the microstructure of Cu has on the local removal rate during CMP. The initial conditions (e.g., grain size, texture,

This is an author-produced, peer-reviewed version of this article. The final, definitive version of this document can be found online published by The Electrochemical Society. Copyright restrictions may apply. doi: 10.1149/1.3254163

and surface topography) and processing steps (e.g., annealing) will directly influence the CMP process. In general, the purpose of CMP is to produce a smooth, flat surface for subsequent processing steps during semiconductor device manufacturing. However, we find that this outcome, especially for thicker films that require a more aggressive CMP step, is not always achieved. Understanding how the microstructure affects the local removal rate, on a grain-by-grain basis, can lead to the development of CMP processes tailored to any initial microstructure.

CONCLUSIONS

One important method to enable three-dimensional die stacking is interconnection by through-wafer vias; in order to completely fill the vias, a thick copper film is deposited and subsequently removed by aggressive CMP. Little work has been done that examines the effects of aggressive CMP on copper and few studies exist that correlate Cu microstructure with CMP output variables like removal rate and surface height variation. Here, results from CMP of solid Cu disks with very large grains to simulate thick electroplated Cu films are presented, and crystallographic orientation is shown to have a role in a grain's resistance to aggressive CMP. Furthermore, texture and grain size of thick films can be altered by varying polarizer concentration in the electroplating bath. By altering bath chemistry between plating runs, samples are created with different microstructures and subsequently CMP is performed. Data from mass change measurements, EBSD, AFM and optical profilometry collected after CMP show bulk removal rate, surface height variation, and microscopic topography are functions of microstructural features such as grain size, crystallographic orientation and grain boundary character. From this work, we conclude:

1. Microstructure has a significant role in the results of CMP, and microstructural parameters like crystallographic texture, grain size, and grain boundary character are strongly influenced by plating bath chemistry.
2. Modifying the grain size of thick electroplated Cu films by annealing increases removal rate during aggressive CMP, yet, for a given grain size, [111] fiber textured samples tend to have lower removal rates during aggressive CMP. This result is likely due to the lower surface energy of (111) surfaces in Cu.
3. In general, the local removal rate is lower for grains whose surface normals are near the [111] direction and increases as the angle between the surface normal and the [111] direction increases, resulting in observed differences in bulk removal rate as a function of crystallographic texture.
4. Grain boundary character affects topographical transitions between grains. While Σ3 twin boundaries are resistant to etching during CMP, general grain boundaries develop grooves that are deeper than either of the neighboring grains. The distribution of grain boundaries in the microstructure can affect the bulk and local removal rate and will lead to different surface topographies depending on grain size.

The exact relationship between the microstructure of Cu and CMP removal rate and surface height is complex because the effects of microstructural parameters are easily confounded during plating and annealing. Further work is required to isolate the effect individual microstructural parameters have on the results of CMP.

ACKNOWLEDGEMENTS

This material is based upon work supported by the Space and Naval Warfare Systems Center under Award Number N66001-05-1-8911. Any opinions, findings, conclusions or recommendations expressed in this publication are those of the authors and do not necessarily

This is an author-produced, peer-reviewed version of this article. The final, definitive version of this document can be found online published by The Electrochemical Society. Copyright restrictions may apply. doi: 10.1149/1.3254163

reflect the views of the Space and Naval Warfare Systems Center. The authors would like to thank Matthew Lueck at RTI for assistance in preparing the electroplated specimens.

REFERENCES

1. J. M. Steigerwald, S. P. Murarka, R. J. Gutmann, *Chemical Mechanical Planarization of Microelectronic Materials*, J. Wiley, New York (1997).
2. S. H. Li, R. Miller, *Chemical Mechanical Polishing in Silicon Processing*, Academic Press, New York, NY (2000).
3. G. B. Shinn, V. Korthuis, A. M. Wilson, in *Chemical–mechanical polishing*, Y. Nishi, R. Doering, editors, p. 415, Marcel Dekker, Inc., New York, NY (2000).
4. D. Temple, M. Lannon, D. Malta, J. E. Robinson, P. R. Coffman, T. B. Welch, M. R. Skokan, A. J. Moll, W. B. Knowlton, Proceedings of the SPIE Defense & Security Symposium. **6544**, 65440 (2007).
5. J. Jozwiak, R. G. Southwick, V. N. Johnson, W. B. Knowlton, A. J. Moll, *IEEE Transaction on Advanced Packaging*, **31**, 4 (2008).
6. S. Spiesshoefer, J. Patel, T. Lam, L. Cai, S. Polamreddy, R. F. Figueroa, S. L. Burkett, L. Schaper, R. Geil, B. Rogers, *J Vac Sci Technol*, **24**, 1277 (2006).
7. P. A. Miranda, J. A. Imonigie, A. J. Moll, *J. Electrochem. Soc.*, **153**, G211 (2006).
8. Y. Ein-Eli, D. Starosvetsky, *Electrochimica Acta*, **52**, 1825 (2007).
9. D. Tabor, *Review of Physics in Technology* **1**, 145 (1970).
10. F. P. Bowden, C. A. Brookes, A. E. Hanwell, *Nature*, **203**, 27 (1964).
11. H. Liang, D. Craven, *Tribology in Chemical-Mechanical Planarization* CRC Press, Boca Raton, FL (2005).
12. W. E. Tragert, W. D. Robertson, *J. Electrochem. Soc.*, **102**, 86 (1955).
13. J. L. Weininger, M. W. Breiter, *J. Electrochem. Soc.*, **110**, 484 (1963).
14. B. E. Sundquist, *Acta Metall.*, **12**, 67 (1964).
15. R. D. Mikkola, Q. T. Jiang, B. Carpenter, *Plating and Surface Finishing*, **87**, 81 (2000).
16. A. K. Sikder, A. Kumar, P. Shukla, P. B. Zantye, M. Sanganaria, *J. Electron. Mater.*, **32**, 1028 (2003).
17. H. P. Feng, J. Y. Lin, M. Y. Cheng, Y. Y. Wang, C. C. Wan, *J. Electrochem. Soc.*, **155**, H21 (2008).
18. A. P. Sutton, R. W. Balluffi, *Interfaces in Crystalline Materials*, Oxford, (1995).
19. P. Shukla, A. K. Sikder, P. B. Zantye, A. Kumar, M. Sanganaria, Proceedings of the 171 (2004).
20. C. Ni, I. W. Hall, T. M. Thomas, J. K. So, J. Quanci, *J. Phys. D*, **37**, 2446 (2004).
21. D. K. Watts, Y. Chiamori, T. Kohama, N. Kimura, Proceedings of the Materials Research Society. **671**, M3.1 (2001).
22. D. Ernur, L. Carbonell, K. Maex, Proceedings of the MRS 2003 Spring Symposium. (2003).
23. S. P. Riege, C. V. Thompson, *Scripta Mater.*, **41**, 403 (1999).
24. D. Ernur, V. Terzieva, W. Wu, S. H. Brongersma, K. Maex, *J. Electrochem. Soc.*, **151**, B636 (2004).
25. H. Zhu, L. A. Tessaroto, R. Sabia, V. A. Greenhut, M. Smith, D. E. Niesz, *Applied Surface Science*, **236**, 120 (2004).
26. C. A. Schuh, K. Anderson, C. Orme, *Surf. Sci.*, **544**, 183 (2003).
27. D. Temple, C. A. Bower, D. Malta, J. E. Robinson, P. R. Coffman, M. R. Skokan, T. B. Welch, Proceedings of the Materials Research Society **970**, Y03.06 (2007).

This is an author-produced, peer-reviewed version of this article. The final, definitive version of this document can be found online published by The Electrochemical Society. Copyright restrictions may apply. doi: 10.1149/1.3254163

28. M. Datta, T. Osaka, J. W. Schultze, *Microelectronic Packaging*, CRC Press, Boca Raton, FL (2005).
29. J. F. Lin, J. D. Chern, Y. H. Chang, P. L. Kuo, M. S. Tsai, *J. Tribol.*, **126**, 185 (2004).
30. D. Ernur, L. Carbonell, K. Maex, Proceedings of the Materials Research Society. **781E**, Z2.7 (2004).
31. X. H. Liu, J. F. Gu, Y. Shen, C. F. Chen, *Scripta Mater.*, **58**, 564 (2008).
32. Y. Liu, S. Varghese, J. Ma, M. Yoshino, H. Lu, R. Komanduri, *Int. J. Plasticity*, **24**, 1990 (2008).
33. T. Tsuru, Y. Shibutani, *Phys. Rev. B*, **75**, 035415 (2007).
34. M. Yamashita, T. Mimaki, S. Hashimoto, S. Miura, *Philos. Mag. A*, **63**, 695 (1991).
35. F. W. Young, Jr., J. V. Cathcart, A. T. Gwathmey, *Acta Metall.*, **4**, 145 (1956).
36. J. V. Cathcart, G. F. Peterson, C. J. Sparks, *J. Electrochem. Soc.*, **116**, 664 (1969).
37. J. Li, J. W. Mayer, E. G. Colgan, *J. Appl. Phys.*, **70**, 2820 (1991).

This is an author-produced, peer-reviewed version of this article. The final, definitive version of this document can be found online published by The Electrochemical Society. Copyright restrictions may apply. doi: 10.1149/1.3254163

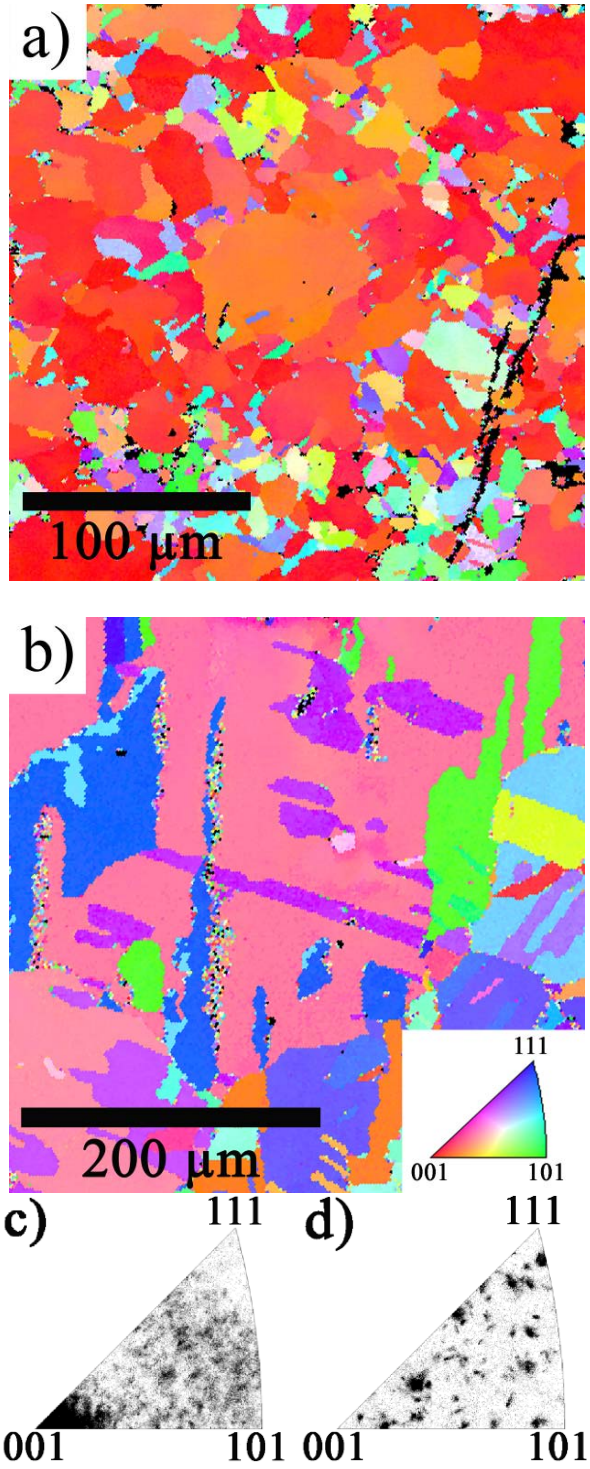

Figure 1: EBSD orientation maps and discrete pole figure maps for: cold-rolled copper as-received (a, c) and cold-rolled copper annealed for 16 h at 700°C (b, d). The EBSD inverse pole figure map shows the crystallographic orientation for each point in the sample area and the inset legend gives the color that corresponds to each surface normal. The discrete pole figure plots have a single point representing each point in the scan area and are a more quantitative representation of crystallographic texture.

This is an author-produced, peer-reviewed version of this article. The final, definitive version of this document can be found online published by The Electrochemical Society. Copyright restrictions may apply. doi: 10.1149/1.3254163

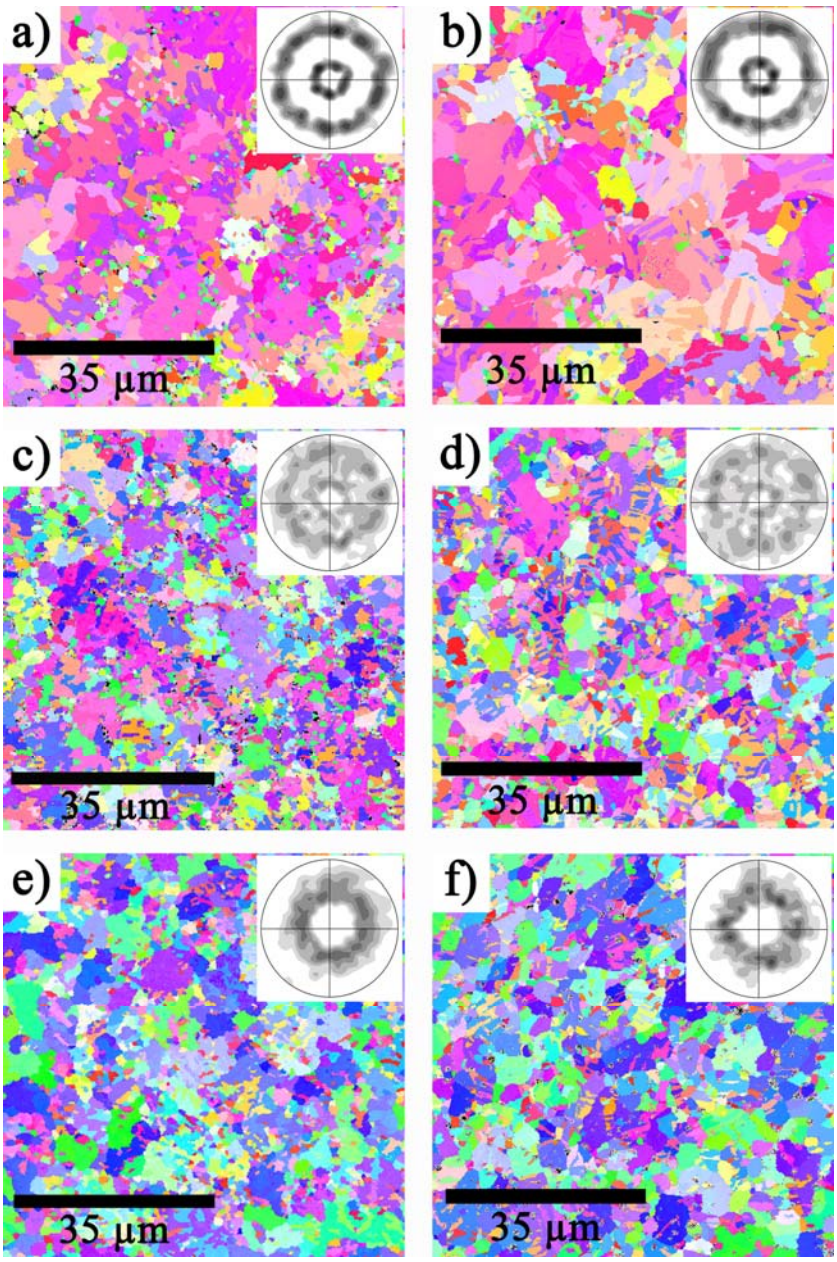

Figure 2: EBSD orientation maps for electroplated Cu films that have different concentrations of polarizer bath additives: (a, b) 0 mL/L, (c, d) 1 mL/L, (e, f) 7 mL/L. Maps in the left column (a, c, e) are for as-plated specimens and maps in the right column (b, d, f) are for specimens annealed for 2 h at 400°C. The EBSD inverse pole figure map shows the crystallographic orientation for each point in the sample area; the colors are the same as in Figure 1. The insets show pole figures that illustrate the crystallographic texture of the specimen. The color contours have the same values for all plots in units of multiples of a random distribution (MRD). From white to black, the contour levels are 0.76, 1.00, 1.32, 1.74, 2.30, 3.03, 4.00 MRD.

This is an author-produced, peer-reviewed version of this article. The final, definitive version of this document can be found online published by The Electrochemical Society. Copyright restrictions may apply. doi: 10.1149/1.3254163

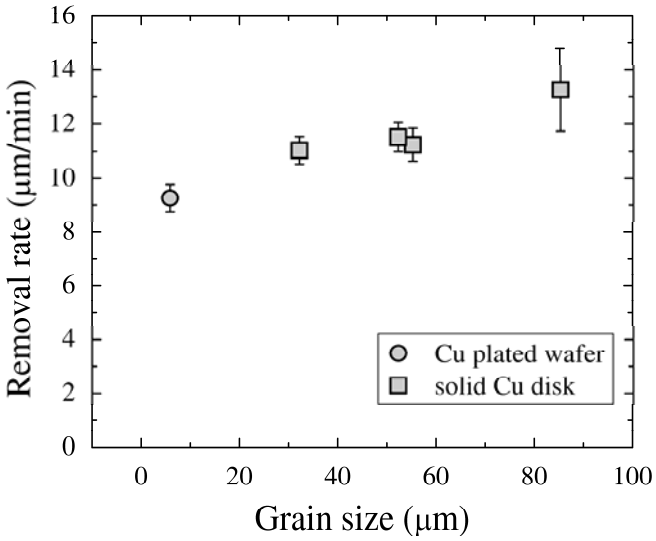

Figure 3: Removal rate during CMP using an undiluted slurry of a Cu plated wafer and copper disk specimens as a function of grain size. Each point represents the mean from a set of three measurements and the error bars represent one standard deviation.

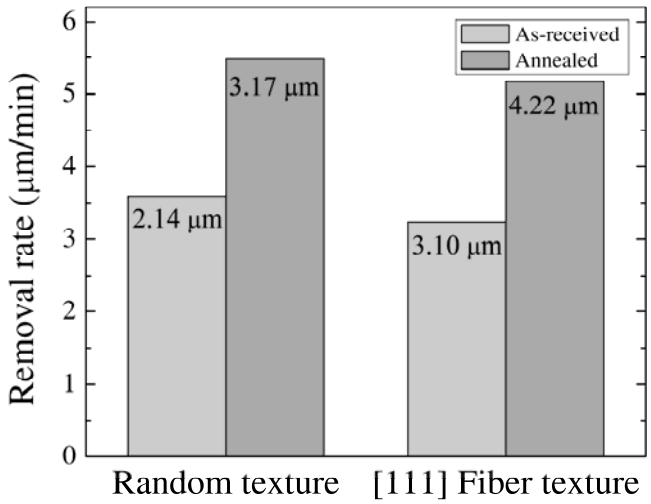

Figure 4: Removal rates before and after annealing for electroplated Cu films with a random texture (left) and a [111] fiber texture (right). CMP was performed with a diluted slurry. The grain size for each specimen is indicated on the bar.

This is an author-produced, peer-reviewed version of this article. The final, definitive version of this document can be found online published by The Electrochemical Society. Copyright restrictions may apply. doi: 10.1149/1.3254163

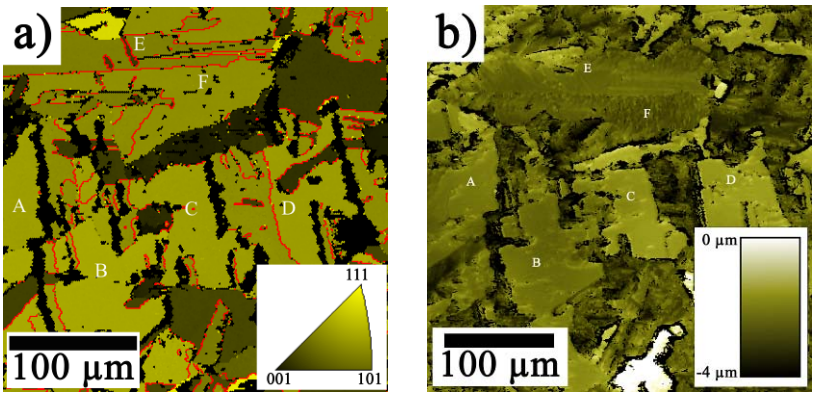

Figure 5: EBSD orientation map (left) and optical profilometry map (right) for an annealed solid copper disk that has undergone aggressive CMP. The EBSD inverse pole figure map shows the crystallographic orientation for each point in the sample area and the inset shows the legend for surface normal direction in the standard stereographic triangle; legend colors have been altered to show grains with surface normals oriented further from [111] as darker. The optical profilometry map shows the surface height for each point in the sample area. The oxide height legend gives surface height where increasing heights are lighter in color.

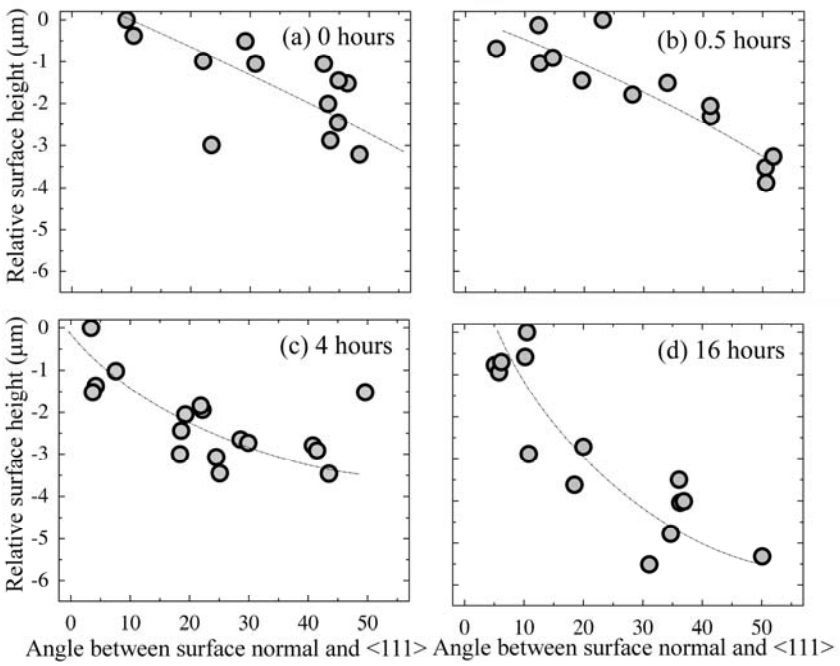

Figure 6: The relative surface height of individual grains after aggressive CMP is plotted as a function of deviation of the grain's surface normal from a <111> direction. Each point represents a single grain from the specimen surface. Plots show results from solid copper disks annealed at 700°C for (a) 0 h, (b) 0.5 h, (c) 4 h, and (d) 16 h. Lines are shown to illustrate a general trend and are not fitted curves.

This is an author-produced, peer-reviewed version of this article. The final, definitive version of this document can be found online published by The Electrochemical Society. Copyright restrictions may apply. doi: 10.1149/1.3254163

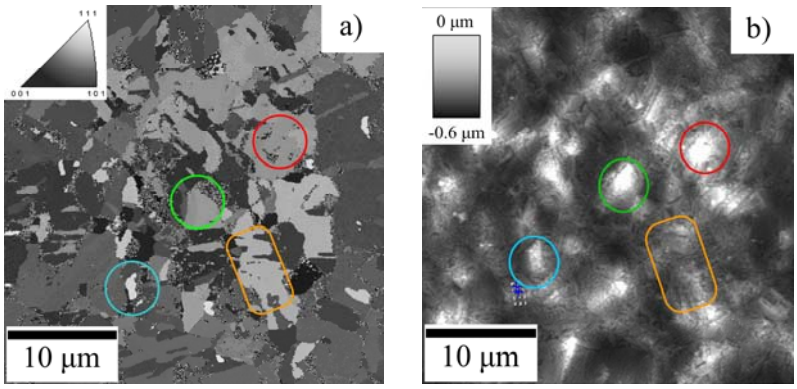

Figure 7: (a) EBSD orientation map and (b) optical profilometry map for an annealed electroplated wafer (1 mL/L polarizer) that has undergone aggressive CMP. The EBSD inverse pole figure map shows the crystallographic orientation for each point in the sample area and the inset shows the legend for a surface normal in the standard stereographic triangle; legend colors have been set to show grains with surface normals oriented further from [111] as darker. The optical profilometry map shows the surface height for each point in the sample area. Several microstructural features are highlighted in each image to show the correspondence of the two areas.

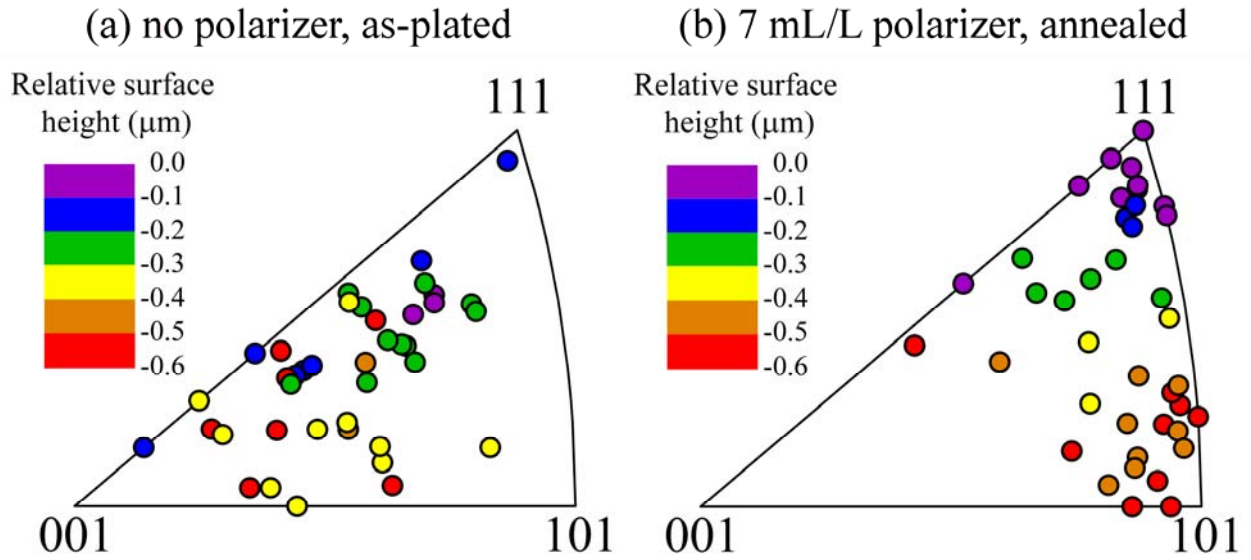

Figure 8: Surface height versus crystallographic orientation for two electroplated Cu film specimens that have undergone aggressive CMP: (a) an electroplated film with no polarizer in the plating bath (c.f., Figure 2a) and (b) an electroplated film with a polarizer concentration of 7mL/L and annealed for 2 h at 400°C (c.f., Figure 2f). Each point in the inverse pole figure map represents an individual grain in the scan area. The position of the point in the inverse pole figure maps gives the orientation, whereas surface height from AFM is indicated by the color of the point.

This is an author-produced, peer-reviewed version of this article. The final, definitive version of this document can be found online published by The Electrochemical Society. Copyright restrictions may apply. doi: 10.1149/1.3254163

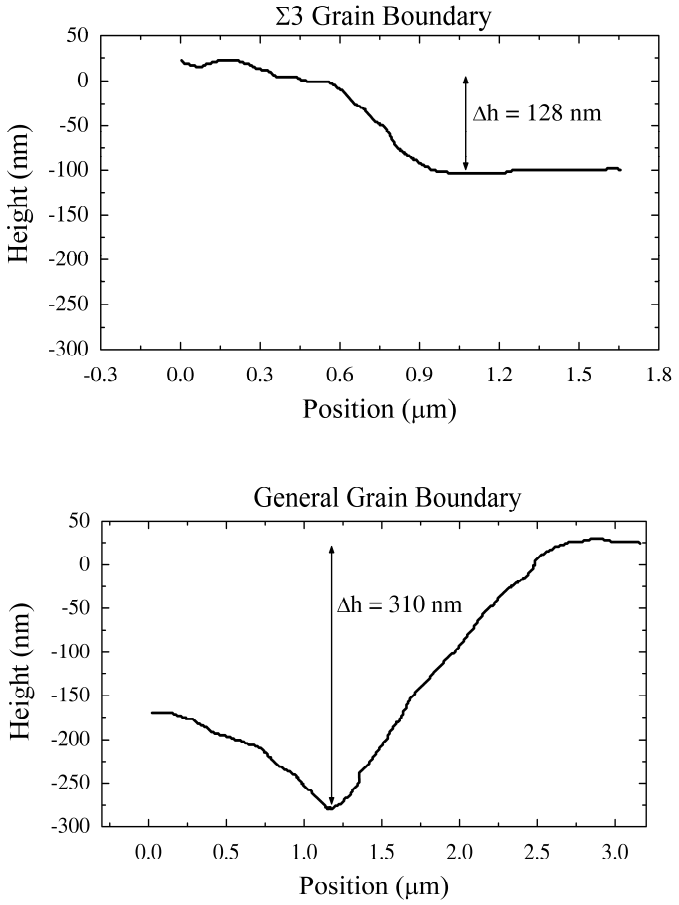

Figure 9: AFM line scans across a Σ3 grain boundary (top), and a general grain boundary (bottom) on an annealed solid copper disk after aggressive CMP. The arrow shows the maximum height difference across the grain boundary.

This is an author-produced, peer-reviewed version of this article. The final, definitive version of this document can be found online published by The Electrochemical Society. Copyright restrictions may apply. doi: 10.1149/1.3254163